Characterization of Beta Zeolites by X-Ray Diffraction, Scanning Electron Microscope, and Refractive Index Techniques

SHER AKBAR
Department of Chemistry, University of Balochistan, Quetta, Pakistan.

(Received on 17th March 2009, accepted in revised form 22nd April 2010)

Summary: Lithium and sodium beta zeolites (Li-BEA, Na-BEA) by aqueous ion exchange at 65 °C and protonic beta zeolite (H-BEA) by deammoniation of NH_4-BEA at 540 °C were prepared. The crystallinity and morphology of all the samples of beta zeolite were examined by X-ray diffraction (XRD) and scanning electron microscopic (SEM) techniques.The hydrophobic and hydrophilic property was measured by refractive index technique. The measurements of the pH of the slurries 4% (g/mL) of parent beta zeolite (NH_4-BEA),H-BEA. cation exchanging slurries and cation exchanged beta zeolites indicated the occurring of the process of ion-exchange. The lowest pH (3.2) was recorded for the ion-exchanging slurry of H-BEA by LiCl and NaCl solutions due to the formation of hydrochloric acid (HCl) during the cation- exchange process. Among the beta zeolites studied the proton form (H-BEA) showed that it was stable in the highly acidic reaction medium.

Introduction

Beta zeolite (BEA) has been known since 1967, when it was reported at Mobil using the tetraethyl ammonium ion (TEA^+) as structure directing agent [1]. Although, beta zeolite has been in use since its discovery, but the models for the structure of beta zeolite were presented in 1988 independently by Higgins *et al* [2], and Newsam *et al* [3]. The structure of beta zeolite is the most complex determined to date and interest was not high until the material became important for some dewaxing operations [4]. This is only a high silica zeolite, which possess a three-dimensional system of large pores and has tetragonal crystal structure with straight 12-membered ring channels (saddle-shape) with cross section of 7.6×6.4 Å with cross tortuous 10-membered ring channels of 5.5×5.5 Å. The framework structure of beta zeolite is shown in Fig. 1. It is disordered in the c-direction [5]. That is, well-defined layers are stacked in a more or less random fashion. Adjacent layers are related to one another by a rotation of 90°. The disorder arises because this rotation can be in either a clockwise or a counter-clockwise sense. If the counterclockwise or clockwise rotations were maintained throughout the crystal, the structure would be ordered and chiral. Whatever, the stacking sequence, a 3-dimensional 12-ring channel system results, so for catalytic applications the stacking sequence is not important.

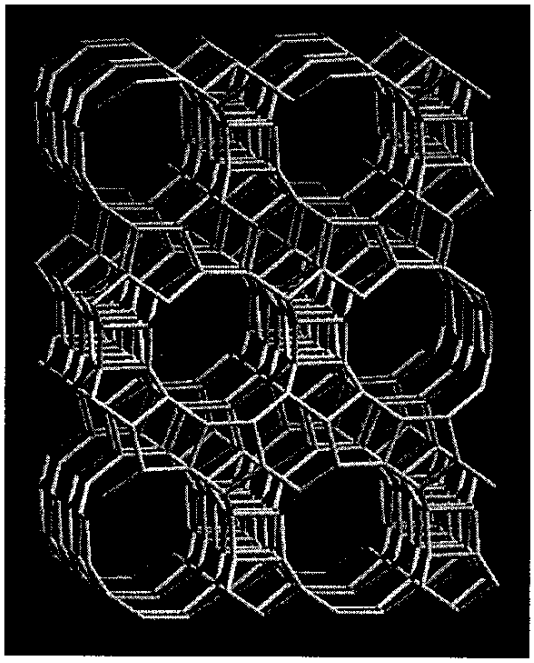

Fig. 1: Framework structure of beta zeolite.

Beta zeolite has a substantial industrial importance [6]. It has been investigated as potential catalyst in the petrochemical industry due to its high acidity, peculiar pore system and high surface area of

the catalyst (> 670 m^2g^{-1}) [7]. The high selectivity of zeolite BEA might originate from suitable acid sites in pores of its defined size and shape [6]. Alkali cation exchange has been mainly used to modify basicity. These applications motivate studies on the structural and thermodynamic properties of various ion exchanged forms of beta zeolite [8]. Further, tuning of the selectivity could be realized by changing cation in a series of alkali-metal exchanged BEA catalysts which is an indication that the reaction proceeds in the micropores [9].

The aim of this work is to prepare Na-BEA and Li-BEA from NH_4-BEA by aqueous ion exchange technique and H-BEA by deammoniation from NH_4-BEA zeolite and then characterize by X-ray diffraction (XRD), scanning electron microscope (SEM) and refractive index techniques in order to check their crystal integrity, morphology and hydrophilic-hydrophobic properties. Furthermore, by measuring the pH of the parent, cation exchanging and cation exchanged zeolite slurries will indicate the occurring of the process of cation exchange reaction.

Results and Discussion

Table-1 lists the pH of the slurries of 4% (g/mL) of all the BEA zeolites and the cation exchanging slurries of the BEA zeolite samples. The table indicates that the parent zeolite (NH_4-BEA) has pH 5.27 and its protonic form (H-BEA) becomes more acidic (pH 4.24). The pH value of H-BEA zeolite suggests the formation of the protonic form of BEA zeolite from deammoniated NH_4-BEA zeolite at 540 °C. The increase in the pH of Li-BEA and Na-BEA zeolites may be due to hydrolysis of $Li^+$and Na^+ into LiOH and NaOH species. Further, the pH of the cation exchanging slurry of H-BEA zeolite is reduced to 3.2 due to formation of hydrochloric acid (HCl) during cation exchange process as given by the following reaction

$$\text{H-BEA}_{(z)}+\text{MCl}_{(s)} \longrightarrow \text{M-BEA}_{(z)} + \text{HCl}_{(sol)}$$

where M= Li^+or Na^+ and the notations (z) and (sol) refer to the ions in the zeolite and in solution phases. It also suggests that BEA zeolite structure is stable in the highly acidic medium [9-11]. When the zeolite cations are protons as in H-BEA the zeolite becomes a strong solid acid. Such solid acids form the foundations of zeolite catalysis applications including the important fluidized bed cat-cracking refining process and isomerization [12-14]. Other types of reactive metal cations can also populate the pores to form catalytic materials with unique properties. Molecules can be separated *via* shape and size effects related to their possible orientation in the pore, or by differences in strength of adsorption [14]

Table-1: pH of the slurries 4 % (g/mL) of the BEA zeolite samples at 65 °C

Zeolite	Parent zeolite	pH of Salt soln MCl	Cation exchanging slurry	Cation exchanged slurry
NH_4-BEA	5.27	—	—	—
Li-BEA[a]	—	6.5	6.5	8.08
Na-BEA[a]	—	6.5	4.5	7.28
H-BEA[b]	4.24	—	—	—
Li-BEA[c]	—	6.5	3.2	6.86
Na-BEA[c]	—	6.5	3.2	6.96

a : $Li^+$and Na^+-exchanged beta zeolite prepared from NH_4-BEA
b: H-BEA prepared by deammoniation from NH_4-BEA
c : $Li^+$and Na^+-exchanged beta zeolite prepared from H-BEA

The XRD patterns of BEA zeolite samples are shown in Fig. 2. The diffraction patterns of the zeolite samples show the reflections in the range 5-35° typical of zeolites [15]. The XRD patterns of the parent zeolite and their corresponding Li^+, Na^+-exchanged products were found identical indicating that the structures of the zeolite remained same during cation exchange. The XRD patterns match very well with those reported by D.Vassena *et al* [9] for H-BEA zeolite. The XRD patterns show high crystallinity of the zeolite samples. The relative crystallinity was evaluated by comparing the area of the characteristic peaks (2θ = 7.7°, 22.5°) of the zeolite samples. The structure of the BEA zeolite is retained during the cation exchange process, as observed from the retention of all characteristic peaks in XRD patterns after the cation exchange process (Fig. 2). The percentage crystallinities of the BEA zeolites are given in Table-2. The XRD patterns reveal the presence of fully crystalline structures of all BEA zeolites except a partial loss of crystallinity of Li-BEA which results in a depression of the XRD peaks intensities which supplies evidence of a partial loss of crystallinity of the zeolite structure.

Table-2: Percentage crystallinity of BEA zeolite samples.

Zeolite	% age Crystallinity
NH_4-BEA	99.99
Li-BEA[a]	71.54
Na-BEA[a]	99.98
H-BEA[b]	99.99
Li-BEA[c]	—
Na-BEA[c]	100

Fig. 3 shows the Scanning Electron Microscope (SEM) images for the samples of BEA zeolite. The morphology of BEA zeolite is nearly round ball with uniform crystal size [16, 17]. The SEM pictures of beta zeolites look rather similar. It has been reported [17] that they do not show any particular cystal habit. Average crystal size is 0.20 μm and the crystal size distribution is very narrow (the size of ~90% of crystal is between 0.10-0.30 μm). Xia *et al* [16] reported that the morphology of BEA zeolite synthesized in fluoride medium can be seriously affected by seeding crystals, crystallization time and silica source. The spontaneous nucleation in fluoride medium resulted in the crystals with especially uniform crystalline morphology, while the presence of BEA zeolite seeding induced mixed crystals consisting of different shapes. Prolonging the crystallization time remarkably increased the crystal size of siliceous BEA. Tetraethylorthosilicate (TEOS) as the silica source resulted in the formation of a single-crystal zeolite BEA, but aerosil-200 silica source induced a multi-crystal BEA. Rao *et al* [17] reported that the particle sizes of Ti-BEA were about 0.2 μm, suggesting that the presence of Ti in gels reduced particles size of the products. This also supports that hetero atoms such as Al and Ti increased the number of nuclei formed, leading to smaller particle size of products. It has been further shown by Rao *et al* [17] that the particle size of BEA increased from 60 to 400 nm, when SiO_2/Al_2O_3 ratio was raised from 30 to 730. The absence of hetero atoms might have reduced the number of nuclei formed leading to the products with larger particle sizes.

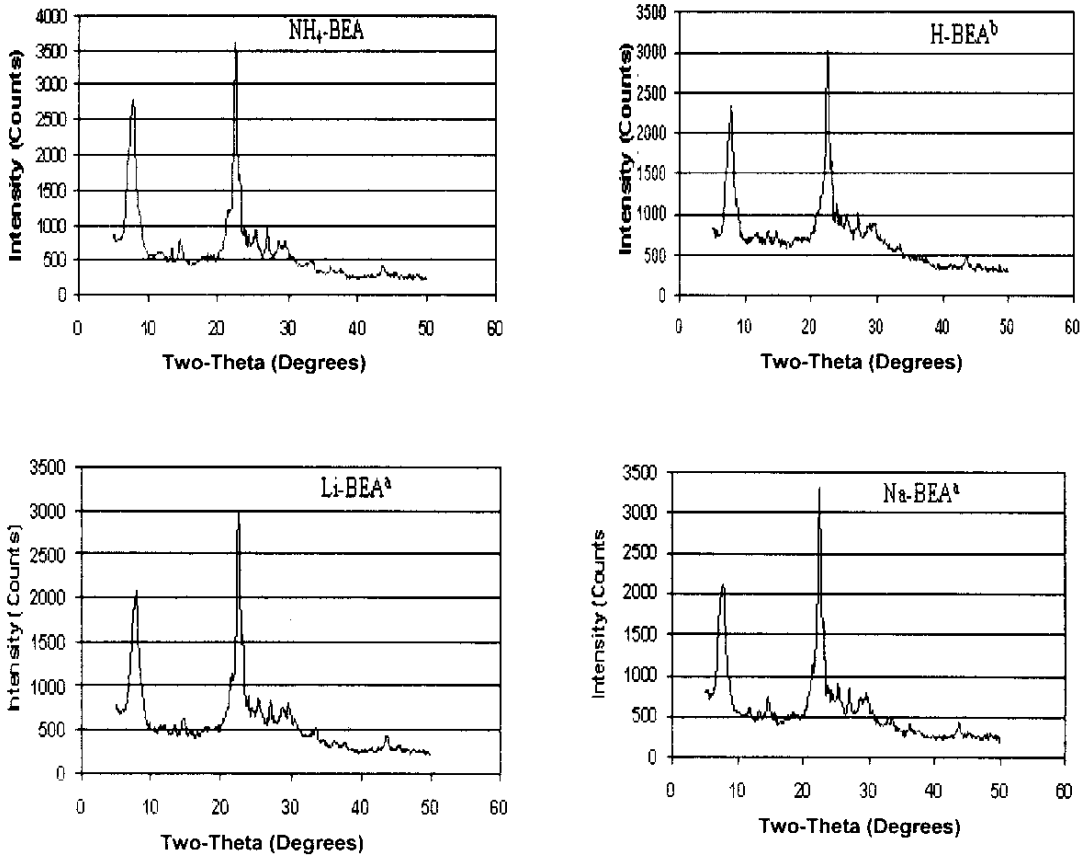

Fig. 2: XRD patterns of beta zeolites

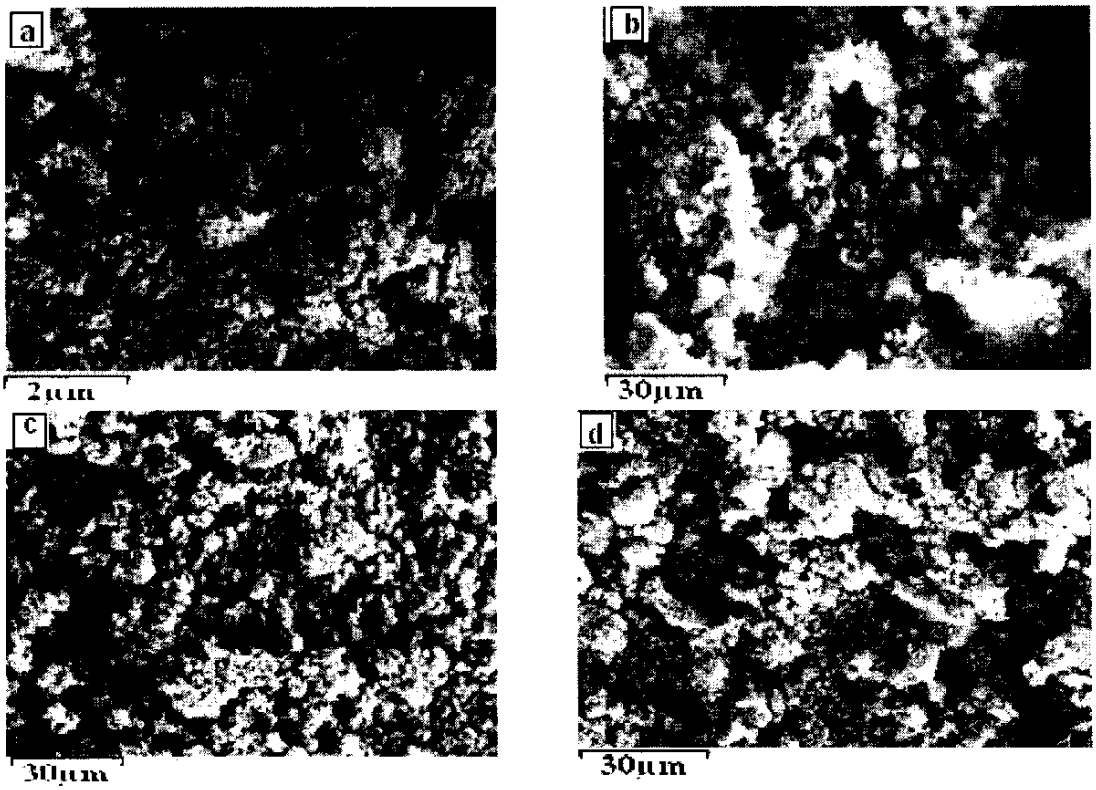

Fig. 3: SEM pictures of beta zeolites. (a) Low (1000×) and (b) higher (15000×) magnification views of H-BEA[b], (c) Li-BEA[a] (low magnification), (d) Na-BEA[a] (low magnification).

The values of refractive indices of aqueous carboxylic acids with and without adsorption into BEA zeolite samples at 20 °C are given in Table-3. The refractive indices of deionised water, formic, acetic and propionic acids were recorded at 20 °C were 1.3346, 1.3719, 1.3715 and 1.3862, respectively. The table shows that the values of refractive indices of supernatants have increased from blank solutions indicating that the samples of BEA zeolite are hydrophilic. The hydrophilicity and hydrophobicity of a zeolite depends mainly on its silica to alumina ratio [18]. Low silica zeolites are hydrophilic whereas high silica zeolites are hydrophobic and the transition occurs around Si/Al ratio of ~10 [19]. As mentioned earlier from the unit cell formula of BEA the Si/Al ratio is 8.14, which is less than 10, therefore it is hydrophilic. As BEA has 7 Al atoms per unit cell, therefore, framework is anionic with its charge balanced by seven extra framework cations (NH_4^+). The negative charge is associated with the $(AlO_{4/2})^-$ tetrahedral that are part of the framework. The negative charge is primarily located at the oxygen atoms ($O^{\delta-}$) surrounding the aluminium atoms. These oxygen atoms are more basic than oxyen bonded to two silicon atoms. The protons are always coordinated to one of these framework oxygen atoms (Si-O-Al-OH-Si) forming Bronsted acid sites. These protons are responsible for the acid properties of the zeolite [20]. These BEA zeolites are hydrophilic because water forms hydrogen bonds with the acid sites (water as H-bond acceptor) and water form hydrogen bonds with the oxygen atoms surrounding the aluminium tetrahedral (as H-bond donor). These protons are labile as evidenced by their ion-exchange properties with other cations such as Li^+ and Na^+ described in the text.

Table-3: Adsorption of Aqueous HCOOH, CH_3COOH and C_2H_5COOH at 20 °C in NH_4-BEA, H-BEA, Li-BEA and Na-BEA zeolites.

Aq.Acid % (V/V)	n_D[d]	Wt (g)	Aq.Acid (mL)	NH_4-BEA n_D	H-BEA[b] n_D	Li-BEA[c] n_D	Na-BEA[c] n_D
HCOOH							
20	1.3467	0.5	5	—	1.3475	1.3475	1.3474
CH_3COOH							
10	1.3400	1.0	10	1.3406	—	—	—
20	1.3489	0.5	10	—	1.3493	1.3491	1.3494
C_2H_5COOH							
16	1.3476	0.25	5	—	1.3483	—	—
20	1.3508	0.25	5	—	1.3508	1.3510	1.3508

d: Refractive indices of solutions at 20 °C.

The NH_4-BEA, H-BEA, Li-BEA and Na-BEA zeolites can have several water molecules depending on the size of extra framework cation and coordinated to the cations in its hydrated form [8, 21]. The water transport through pores is more likely favoured because of a combination of favourable diffusion, due to small size (radius 2.8 Å) of water molecules, and favourable solubility due to hydrophilic ionic species H^+, Li^+, Na^+, and NH_4^+. The exact positions of cations are affected by the local surroundings for example, Si/Al ratio. When there is one aluminium atom in the ring, the cations locate near the oxygen atoms involved in the Al-O-Si bridges. When two or three aluminium atoms are present in the six-membered rings, the cations locate near the center of the ring by interacting with the oxygen atoms that are pointing towards the inside of the ring [22]. Zeolite BEA has an intersecting tube type of pore structure, with free diameters in the tube segments of 5.6-7.5 Å [23]. In addition, molecular sizes of the carboxylic acids *i.e.* formic (~ 3.5 Å diameter in aqueous solution) acetic (~ 4.5 Å) and propionic (~ 5.6 Å) have no effect on adsorption because they are smaller than the beta zeolite pore aperture (7.6×6.4 Å) as confirmed by XRD [24].

Experimental

Starting from the powder form of NH_4-BEA zeolite having an anhydrous unit cell composition of $(NH_4)_7[Al_7Si_{57}O_{128}]$ [25], particle size small was provided by Zeolyst International (Lot # 814-22-Q_3-FD). Na^+ and Li^+-exchanged BEA zeolites were prepared by conventional aqueous ion-exchange method from NH_4-BEA zeolite using predetermined alkali chloride solution as cation source [8]. 3g of NH_4-BEA zeolite was stirred with 75 mL of deionized water on a magnetic stirrer / hot plate at 25 °C and the pH of the slurry recorded by a pH meter (JENCO Portable Digital 608) was first calibrated with buffer solutions of pH 4 and 7. 1 M / 250 mL, MCl (M=Li^+, Na^+) solution was added in parts and the temperature of the slurry was increased to 65 °C. The pH of the cation exchanging slurry was recorded. The cation exchanged slurry was filtered (cat.No.28310-015 VWR brand) by using buchner funnel and water suction pump. The partially cation exchanged BEA zeolite was washed several times with hot (65°C) deionzed water until complete removal of chloride ions in solution (filtrate) was obtained (tested with $AgNO_3$ solution). This exchange procedure was repeated twice, until the maximum level of exchange was achieved. Left the cation exchanged zeolite sample in the buchner funnel for overnight drying. The dried cation exchanged samples were shifted from buchner funnel to porcelain evaporating dish for further drying at room temperature (25 °C) for several days.

The proton form of BEA zeolite was prepared by deammoniation of the parent zeolite (NH_4-BEA) in a tube furnace (Fischer Scientific isotherm Muffle Furnace 650 series)[16,19]. A top mounted exhaust (3/8 inch) port allows convenient venting of the chamber. Took three porcelain evaporating dishes of size, Di×Ht; 90×22 mm capacity 75 mL to each transferred 5g of NH_4-BEA zeolite. The NH_4-BEA zeolite was then transformed to the H-BEA zeolite by calcining in air at 540 °C [9]. The temperature was raised in ramp rate of 10°C min^{-1} up to 540 °C and the sample was kept at the final temperature for 12 h. Over the course of this process the zeolite should turn from a white to brown / black to an off-white colour. Cooled the material and placed in the fuming cupboard to preserve the acid hydrogen form of the BEA zeolite.

$$NH_4\text{-BEA} \xrightarrow[12\,h]{540^{\circ}C} \text{H-BEA} + NH_3 \qquad *$$

Li-BEA and Na-BEA zeolites were also prepared from H-BEA by aqueous ion exchange technique as described above. The pH of the slurries 4% (g/mL) of the parent, ion exchanging and ion * exchanged samples were also recorded.

The structural integrity and crystallinity of the parent and ion exchanged zeolites at ambient temperature were examined by the powder X-ray

diffraction (XRD) using Rigaku Dmax-A diffractometer with a Ni filtered Cu K_α radiation (λ=1.5406Å) and compared with a highly crystalline standard sample. The XRD data were collected from 5 to 50° (2θ) with a scanning rate of 2° (2θ)/min.

Scanning Electron Microscope (SEM) images were taken using a Hitachi S-4500 cFEG SEM instrument operated at 5 kV, current 10 μA, condenser lens 1-5 mm, working distance 10 mm and aperture 2.

Adsorption experiments were carried out in a screw cap septum vial, 14 mL (L×Dia; 72×18 mm) at room temperature (25 ± 0.5). A known weight of the adsorbents 0.25-1.0g without activation was introduced into 5-10 mL binary solution carboxylic acids and water. The mixture was stirred with an egg-shaped stir bar (L × Dia; 19×9.5) teflon coated on magnetic stirrer / hot plate for about one hour. Then it was left for about 24 hours for settling the suspension until transparent supernatant appeared. The blank solutions were also stirred similarly but without the zeolite samples. 100 μL of the transparent solution was removed by a micro liter syringe and placed on the prism of a refractometer (Reichert AR 200 Digital Refractometer, Germany).The refractive indices of the aqueous solution of carboxylic acids and also blank solutions were recorded. As refractive indices are very sensitive to the temperature, therefore, they were converted to 20°C by using the following formula.

$$n_D^{20} = n_D^{obs} + (t^\circ C - 20)\ 0.00045$$

Conclusions

The intensities of the XRD peaks confirmed the high crystallinity of the BEA zeolite framework structures. The SEM images showed the uniform round shape small crystals of the zeolites. The refractive indices indicated the hydrophilic character of the BEA zeolites, which is attributed due to ratio of Si/Al <10. The pH values of the slurries of the BEA zeolite samples indicated the structural stabilities of the zeolites in acidic medium. The Bronsted acidity was responsible for the low pH of the BEA zeolite samples except Li-BEA and Na-BEA (prepared from NH_4-BEA) where the pH more than 7 suggested the formation of LiOH and NaOH species.

Acknowledgements

The author thanks Megan Pukala for performing XRD and SEM experiments and Dr. R.Q. Snurr of Northwestern University, Evanston, IL,U.S.A. for fruitful discussion and encouragement throughout this research work. The author is also indebted to U.S. Department of State Bureau of Educational and Cultural Affairs for award of Fulbright Post-doctoral fellowship and University of Balochistan, Quetta for granting sabbatical leave.

References

1. R .L Wadlinger, G. T. Kerr, and E. J. Rosinski, *U. S. Patent* 3308069, (1967).
2. J. B. Higgins, R. B. Lapierre, J. L. Schlenker, A. C. Rohrman, J. D. Wood, G. T. Kerr, and W. J. Rohrbaugh, *Microporous and Mesoporous Materials*, **8**, 446 (1988).
3. J. M. Newsam, M. M. J. Treacy, W. T. Koetsier, and C. B. de Grruyter, *Proceedings Royal Society, London, A*, **420**, 375 (1988).
4. T. F. Degnan Jr., *Topics in Catalysis*; **13**, 349 (2000).
5. L. B. McCusker, and C. Baenlocker, In: J. Cejka and H. Van Bekkum (Eds.), *Studies Surface Science Catalysis*; **157**, 41 (2005).
6. C. Yang, J. Wang, and Q. Xu, *Microporous Materials*, **11**, 261 (1997).
7. S. Bernascon, G. D. Pirngruber, A. Kogelbauer, and R. Prins, *Journal of Catalysis*, **219**, 231 (2003).
8. P. Sun, S. Deore, and A. Navrotsky, *Microporous and Mesoporous Materials*, **91**, 15 (2006).
9. D. Vassena, D. Malossa, A. Kogelbauer, and R. Prins, In: M. J. Treacy, B. K. Marcus M. E. Bisher, and J. B. Higgins (Eds.) *Proceedings of the 12th International Zeolite Conference, Materials Research Society*, Warrendale PA, 1471 (1999).
10. H. Lechert, In H. Robson (Ed.) *Verified Synthesis of Zeolitic Materials*, 33 (2001)
11. J. Scherzer, In *ACS Symposium Series*, **248** *American Chemical Society, Washington*, D.C. 157 (1984).

12. L. Ha, J. Mao, J. Zhou, Z. C. Zhang, and S. Zhang, *Applied Catalysis A: General*, **356**, 52 (2009).
13. F. D. Renzo, and F. Fajula, In: J. Cejka, and H. Van Bekkum (Eds.) *Studies Surface Science Catalysis*; **157**, 1 (2005).
14. C. Song, J. M. Garces, and Y. Sugi, In Shape-Selective Catalysis, Chemical Synthesis and Hydrocarbon Processing, *ACS Symposium Series*, **738**, *American Chemical Society*, 1 (2000).
15. J. Sebastian, S. A. Peter, and R. V. Jasra, *Langmuir*, **21**, 11220 (2005).
16. Q. H. Xia, J. Song, S. Kawi, and L. L. Li, In: E. Van Steen, L. H. Callanan, and M. Claeys (Eds.) *Studies Surface Science Catalysis*, **154**, 195 (2004).
17. P. R. Hari Prasad Rao, K. Ueyama, E. Kikuch, and M. Matsukata, In: M. J Treacy, B. K. Marcus, M. E. Bisher, and J. B. Higgins (Eds.), *Proceedings of the 12th international Zeolite Conference, Materials Research Society, Warrendale PA*, 1471 (1999).
18. N. Y. Chen, *Journal of Physical Chemistry*, **80**, 60 (1976).
19. P. Payara, and P. K. Dutta, In: S. M. Auerbach, K. A Carrado, and P. K. Dutta (Eds.). *HandBook of Zeolite Science and Technology*, Marcel Dekker, In: N. Y. Basel 1 (2003).
20. H. Matsuura, N. Katada, and M. Niwa, *Microporous and Mesoporous Materials*, **66**, 283 (2003).
21. M. Cook, and W. C. Conner, In: M. J. Treacy, B. K. Marcus, M. E. Bisher, and J. B. Higgns (Eds.), *Proceedings of the 12th International Zeolite Conference, Materials Research Society, Warrandale* PA, 409 (1999).
22. G. N. Vayssilov, M. Staufer, T. Belling, K. M. Neyman, H. Knozinger, and N. J. Rosch, *Journal of Physical Chemistry* B, **103**, 7920 (1999).
23. J. F. Denyar, W. Souverijns, P. A. Jacobs, J. A. Martens, and G. V. Baron, *Journal of Physical Chemistry B*, **102**, 4588 (1998).
24. V. S. Gurin, and V. P. Petranouskii, In: E. Van Steen, L. H. Callanan, and M. Claeys (eds.), *Studies Surface Science Catalysis*, **154**, 1661 (2004).
25. A. P. Singh, S. P. Mirajkar, and S. Sharma, In; M. J. Treacy, B. K. Marcus, M. E. Bisher and J. B. Higgins (Eds.), *Proceedings of the 12th International Zeolite Conference Materials Research Society*, Warrendale PA, 2203 (1999).